Journal of Solid State Chemistry 181 (2008) 1936–1942

Contents lists available at ScienceDirect

Journal of Solid State Chemistry

journal homepage: www.elsevier.com/locate/jssc

CTAB-assisted synthesis of mesoporous F–N-codoped TiO_2 powders with high visible-light-driven catalytic activity and adsorption capacity

Yi Xie *, Xiujian Zhao *, Yuanzhi Li, Qingnan Zhao, Xuedong Zhou, Qihua Yuan

Key Laboratory of Silicate Materials Science and Engineering, Wuhan University of Technology, Ministry of Education, Wuhan, Hubei 430070, PR China

ARTICLE INFO

Article history:
Received 30 December 2007
Received in revised form
14 April 2008
Accepted 24 April 2008
Available online 3 May 2008

Keywords:
Mesoporous TiO_2
F–N-codoping
Visible light
Photocatalysis
Surfactant
Adsorption

ABSTRACT

This article describes the preparation of mesoporous rod-like F–N-codoped TiO_2 powder photocatalysts with anatase phase via a sol–gel route at the temperature of 373 K, using cetyltrimethyl ammonium bromide (CTAB) as surfactant. The as-prepared photocatalysts were characterized by X-ray diffraction (XRD), scanning electron microscopy (SEM), transmission electron microscopy (TEM), X-ray photoelectron spectroscopy (XPS) and UV–visible diffuse reflectance spectra (UV–vis DRS). The results showed that the photocatalysts possessed a homogeneous pore diameter and a high surface area of 106.3–160.7 $m^3 g^{-1}$. The increasing CTAB reactive concentration extended the visible-light absorption up to 600 nm. The F–N-codoped TiO_2 powders exhibited significant higher adsorption capacity for methyl orange (MO) than that of Degussa P25 and showed more than 6 times higher visible-light-induced catalytic degradation for MO than that of P25.

1. Introduction

Mesoporous inorganic materials [1–5] with high surface area, high damping capacity, low thermal conductivity and low dielectric permittivity have gathered increasing attention because of their potential application in the areas of separations, catalysis, sensing and power generation. Among them TiO_2 is one of the most widely used and investigated inorganic materials because of its nontoxicity, inexpensiveness, chemical stability and favorable optoelectronic properties. Mesoporous TiO_2 synthesized using a sol–gel route was first reported by Antonelli and Ying [6]. Using sol–gel and dip-coating methods, Dionysiou and co-workers [7] also synthesized mesoporous photocatalytic TiO_2 films with high surface area (147 $m g^{-1}$) and porosity (46%) and narrow pore size distribution. Their samples showed high photocatalytic activity for the destruction of methylene blue and creatinine in water. Sakai and co-workers [8] reported the preparation of crystalline mesoporous TiO_2 and they found that the crystallization of TiO_2 from amorphous to anatase form was caused by heating at the temperature of 333 K.

However, the use of TiO_2 photocatalytic technology was hampered because of its large band gap. To solve this problem, considerable efforts have been taken, including dye sensitization [9] and transition metals [10] or nonmetals doping or modifying [11–17]. Among them, nonmetal F/N mono-doping and F–N-codoping of TiO_2 have been viewed as effective ways to lower the band gap of TiO_2 and the consequent high photocatalytic activity for degradation of organics under visible light illumination. Asahi and co-workers [11] reported that TiO_2 doped with nitrogen by sputtering N_2/Ar mixtures extended the spectral absorption into visible region below 500 nm and thus improved the photoelectrochemical reactivity of TiO_2 films toward organic molecules under visible light illumination. Beranek and Kisch [13] prepared N-doped titania films and their samples exhibited photocurrents in the visible down to 700 nm. Dékány and co-workers [15] prepared phoshpate-modified TiO_2 by using sol–gel method and they found that the photocatalytic activity of the modified sample was higher than that of P25 TiO_2. The first report on N–F-codoped TiO_2 was made by Nukumizu and co-workers [18], who prepared $TiN_xO_yF_z$ with a band gap absorption edge at ~570 nm using $(NH_4)_2TiF_6$, SiO_2 and NH_3 as sources. In our previous work [19] we have also prepared F–N-codoped TiO_2 photocatalysts with high visible-light-induced catalytic activity for decompositions of methyl orange (MO).

To our knowledge, however, the effect of surfactant such as cationic surfactant cetyltrimethyl ammonium bromide (CTAB) on the structures and properties of F–N-codoped TiO_2 has rarely been reported. Herein, we describe a detailed synthesis of mesoporous F–N-codoped TiO_2 powders, changing the dosage of surfactant CTAB ($C_{19}H_{42}BrN$). We hope the present method may open a new horizon for the preparation of mesoporous nonmetal-doped TiO_2

* Corresponding authors. Fax: +86 27 8766 9729.
E-mail addresses: xieyithanks@163.com (Y. Xie), opluse@whut.edu.cn (X. Zhao).

0022-4596/$ - see front matter © 2008 Elsevier Inc. All rights reserved.
doi:10.1016/j.jssc.2008.04.021

photocatalysts to use in the organic compounds adsorption and degradation under visible irradiation.

2. Experimental

2.1. Photocatalyst synthesis

F–N-codoped TiO_2 photocatalysts were synthesized using a sol–gel route (Fig. 1). Typically, $TiCl_4$ was added dropwise into 500 mL distilled water in an ice-water bath with strong magnetic stirring. After 30 min, the pH of this acidic solution was adjusted to 7 by dropwise addition of diluted ammonia solution (1:9). After stirring at this pH for 24 h, the obtained white precipitates were filtered and washed thoroughly with distilled water repeatedly until Cl^- ions were not detected. Thereafter the precipitates were ultrasonic dispersed in 500 mL distilled water. H_2O_2 (30%, 50 mL) was added dropwise into this mixture under stirring to obtain yellow semitransparent peroxo-titanic acid (PTA) solution. A total of 0.815 g of NH_4F (Shanghai Shiyi Chemicals Reagent Co., Ltd. China) was added into 100 mL of distilled water followed by the addition of CTAB (Shanghai Bio Life Science & Technology Co., Ltd, China). Then, 400 mL of peroxo-titanic acid solution prepared above was added dropwise into the NH_4F aqueous solution (the starting molar ration of NH_4F/Ti was 3/5). The mixtures were heated at 100 °C for 6.5 h in a temperature controlled oil bath equipped with a magnetic stirrer, thermometer and reflux condenser. The resulting precipitates were washed by ethanol to remove the possible CTAB. Finally, the yellow F–N-codoped TiO_2 powder was obtained after drying the above washed precipitates. The preparation conditions along with other physical properties are presented in Table 1. For comparison, commercial Degussa P25 was selected as reference sample.

2.2. Characterization techniques

Structure phase analysis with the X-ray diffraction (XRD) method was performed on a Rigaku D/MAX-IIIA X-ray diffractometer with Cu$K\alpha$ radiation at 40 kV and 60 mA. A continuous scan mode was used to collect 2θ with a small angle of 0.5–4° and wide angle of 20–70°. The average crystallite sizes were calculated from the peak widths using the Scherrer equation [20].

$$D_{k\,h\,l} = k\lambda(\beta \cos\theta)$$

where $D_{h\,k\,l}$ is the crystallite size, k is the shape factor (a value of 0.89 was used in this study), β is the line width at half-maximum height of the main intensity peak after subtraction of the equipment broadening. λ and θ are the X-ray radiation wavelength (1.5418 Å for Cu$K\alpha$) and Brag angle, respectively. Morphologies of the F–N-codoped TiO_2 particles were examined by the transmission electron microscopy (TEM) (JEM-2010, Japan) operating at 200 kV in the mode of bright field and the scanning electron microscopy (SEM). The specimens for TEM were prepared by dropping an ethanol suspension of the powder onto an amorphous carbon foam, supported by a Cu grid. The specimen was allowed to dry under air at room temperature for 20 min. The SEM observations have been carried out with a Hitachi FE S-4800 (Hitachi Ltd., Japan) at an acceleration voltage of 20 and 15 kV. The UV–visible diffuse reflectance spectra (UV–vis DRS) was recorded on a UV–vis spectrophotometer (UV-2550, Shimadzu, Japan) with an integrated sphere attachment. $BaSO_4$ was used as the reflectance standard.

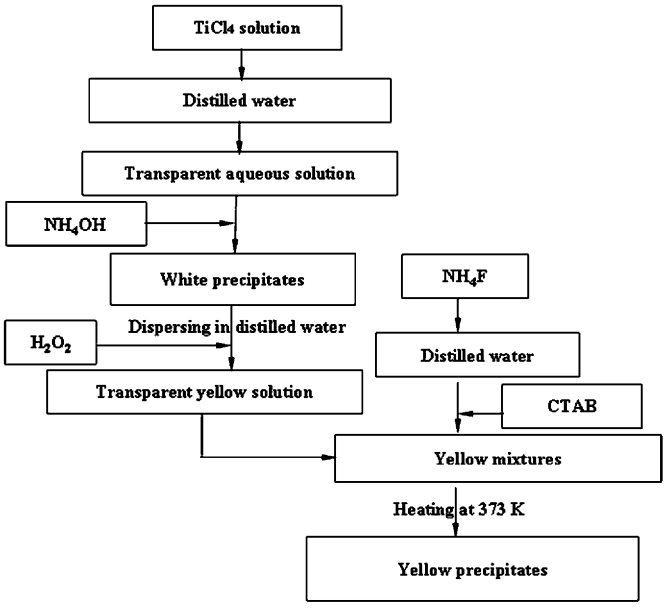

Fig. 1. Schematic diagram of the synthesis of F–N-codoped TiO_2.

2.3. Activity measurements

The evaluation method of photocatalytic activity was undertaken by the degradation of MO using irradiation of a 125 W high-pressure mercury lamp with a UV cut-off filter ($\lambda \geqslant 420$ nm) similar with that reported previously [19], but there are three differences: first, the mixtures of F–N-codoped TiO_2 photocatalysts and MO solution were magnetically stirred for 30 min in the dark before switching on light; second, the incident intensity to the sample surface was 181 $\mu W\,cm^{-2}$; third, the volume of MO solution was 40 mL. The UV–vis spectra of MO solution were recorded on a UV-1601 UV–vis spectrophotometer (Rigaku, Japan).

3. Results and discussion

3.1. Catalyst characterization

Fig. 2 provides the XRD patterns of the F–N-codoped TiO_2 photocatalysts, corresponding to samples A–E in Table 1 from the top to the bottom, respectively. All the samples present distinctive peaks centered at $2\theta = 25.14°$, 37.88°, 47.73°, 53.93°, 62.44° (Fig. 2a), which correspond to the anatase (101), (103, 004 and 112), (200), (105 and 211), (204) crystalline planes (JCPDF: 21-1272). Moreover, the intensity of (101) peak increases with increasing CTAB concentration, which indicates that the addition of CTAB enhances the crystallization of F–N-codoped TiO_2. By using the width of the anatase diffraction peak and the Scherrer equation, the average crystallinity sizes ($D_{k\,h\,l}$) were estimated to have values from 10.9 to 14.2 nm, increasing with the augment of CTAB concentration.

Fig. 2b shows small-angle XRD patterns of F–N-codoped samples prepared with different CTAB concentrations. A peak at ~0.58° with a d-spacing of ~14 nm along with a broad shoulder in the range of ~0.61–1.90° is observed. This result was similar with that reported by Peng and co-workers [21] and was considered to be related to the uniform pore size, which further proved that the resulted photocatalysts had mesoporous structure. Sakai and co-workers [22] prepared mesoporous titania particles using CTAB as surfactant. The diffraction patterns for their samples had three diffraction peaks at around $2\theta = 2.2°$, 3.8°, and 4.2°, which were assigned to the hexagonal mesoporous structure. Cassiers and co-workers [23]

Table 1
Preparation conditions, textural properties and other physical parameters of the F– N-codoped TiO_2 powders

Sample	Starting CTAB concentration (mM)	D_{hkl}[a] (nm)	S_{BET}[b] ($m^2 g^{-1}$)	V_p[c] ($cm^3 g^{-1}$)	D_p[d] (nm)	Relative coefficient[e] (R)	Rate constant[f] (k) (h^{-1})
A	0	10.9	106.3	0.2958	11.1	0.996	0.038
B	0.1	11.5	143.7	0.4000	11.1	0.998	0.227
C	1.0	11.8	143.4	0.3362	9.4	0.999	0.367
D	10	12.5	160.7	0.4785	11.9	0.999	0.426
E	40	14.2	117.5	0.3562	12.1	0.997	0.394

[a] Crystallite size calculated by Scherrer equation.
[b] BET specific surface area.
[c] Total pore volume at $P/P_0 = 0.99$.
[d] Average pore diameter ($4V_p/S_{BET}$).
[e] Photocatalytic degradation relative coefficients for all the products were close to 1, suggesting that the degradation of MO in the presence of the photocatalysts was first-order kinetics reaction.
[f] Photodegradation reaction rate constants.

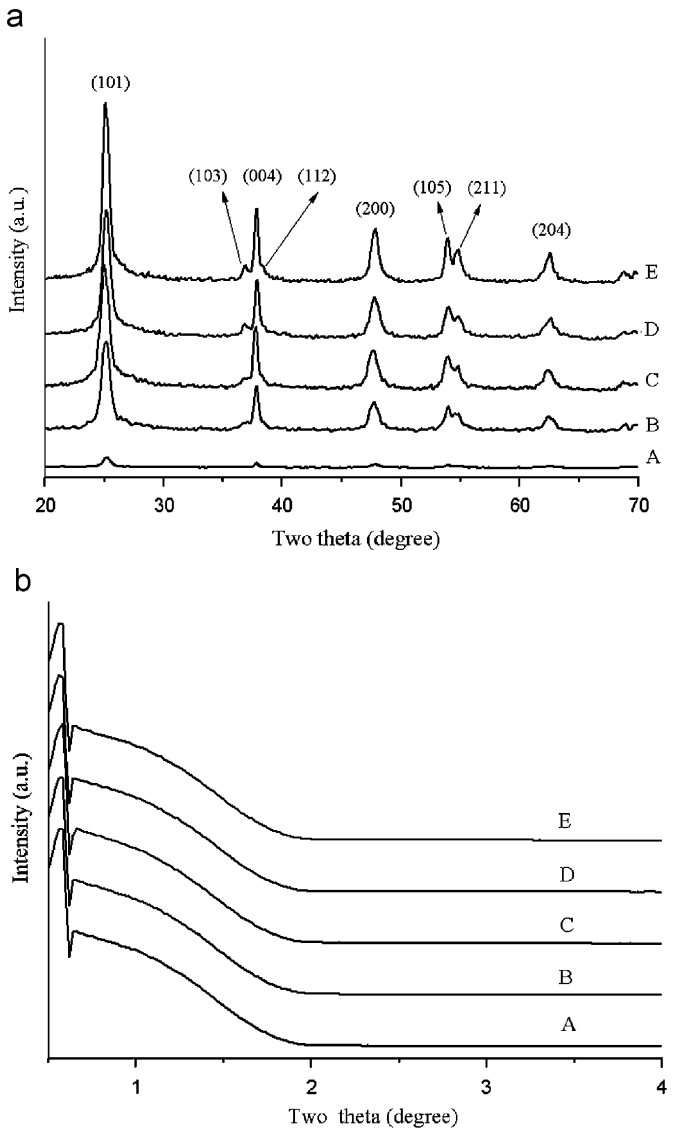

Fig. 2. Wide-angle (a) and low-angle (b) XRD patterns of F–N-codoped TiO_2 prepared with different starting CTAB surfactant: (A) 0 mM, (B) 0.1 mM, (C) 1.0 mM, (D) 10 mM and (E) 40 mM.

also used CTAB as surfactant to prepare mesoporous titania and they attributed the XRD pattern in the 2θ range 2–4° to a pore center to pore center correlation length.

The mesoporous structure of the as-prepared samples can be obviously confirmed by FE-SEM, as shown in Fig. 3. The rod-like F–N-codoped TiO_2 particles were not close-packed enough and took on an overlapped worm-like structure. The pore size was in the range of 20–40 nm, typically the mesoporous structure [24]. This F–N-codoped TiO_2 network with homogeneous, mesoporous structures is beneficial to enhancing the adsorption of reactants and thus improves the photocatalytic activity.

TEM images (Fig. 4a, c) also show that F–N-codoped TiO_2 photocatalysts present crystals with uniform rod-like shapes (length: width ratio of ~4:1). Furthermore, the selected area electron diffraction pattern (Fig. 4b, d) allows that the crystallized codoped samples to be indexed to the anatase phase, which coincides with the analysis of XRD. As reported [25,26], the TiO_2 crystalline shape could be controlled by the addition of surfactant. Weller and co-workers [25] reported the controlled growth of anatase TiO_2 nanorods via hydrolysis of titanium tetraisopropoxide using oleic acid (OLEA) as surfactant at the temperature of 353 K. Using lauric acid (LA, $CH_3(CH_2)_{10}COOH$) as the selective surfactant and trioctylphosphine oxide (TOPO, $[CH_3(CH_2)_7]_3PO$) as the nonselective surfactant, Jun and co-workers [26] prepared TiO_2 anatase nanocrystals. They found that the shape of the TiO_2 nanocrystals could evolve from sphere to bullet, diamond, rod, and branched rod by changing the ratio of the surfactant.

N_2 adsorption–desorption measurement at liquid N_2 temperature of 78 K was also used to study mesoporosity of the samples. The isotherms of the samples (Fig. 5) were of typical type IV, confirming that the as-synthesized powders were mesoporous structures [27,28]. A sharp increase in adsorption volume of N_2 was observed and located in the P/P_0 range of 0.50–0.86. This sharp increase can be attributed to the capillary condensation, indicating the good homogeneity of the sample and fairly small pore size [29]. All of the samples exhibited high surface areas in the range of 106.3–160.7 $m^2 g^{-1}$ (Table 1) and narrow mesopore distributions (Fig. 6). The mesoporous photocatalysts possessed mean pore diameter and total pore volume of 9.4–12.1 nm (within mesopore region) and 0.2958–0.4785 $cm^3 g^{-1}$, respectively. The addition of CTAB changed little the morphology of F–N-codoped crystals but slightly affected the surface area and pore sizes. The samples prepared with the addition of CTAB possessed slightly higher pore volumes and pore diameters, while the F–N-codoped TiO_2 prepared with the CTAB concentration of 40 mM exhibited less surface area and pore volume but larger pore size.

The surfactant CTAB has been reported to be effective in the preparation of mesoporous TiO_2 photocatalysts [30,31]. It was reported that the presence of the counterion of the surfactant was important to keep the nanoordered crystal size unchanged, and hexagonal mesoporous TiO_2 with crystalline wall could be synthesized via optimizing the composition of $TiOSO_4$ and $C_{16}TAB$

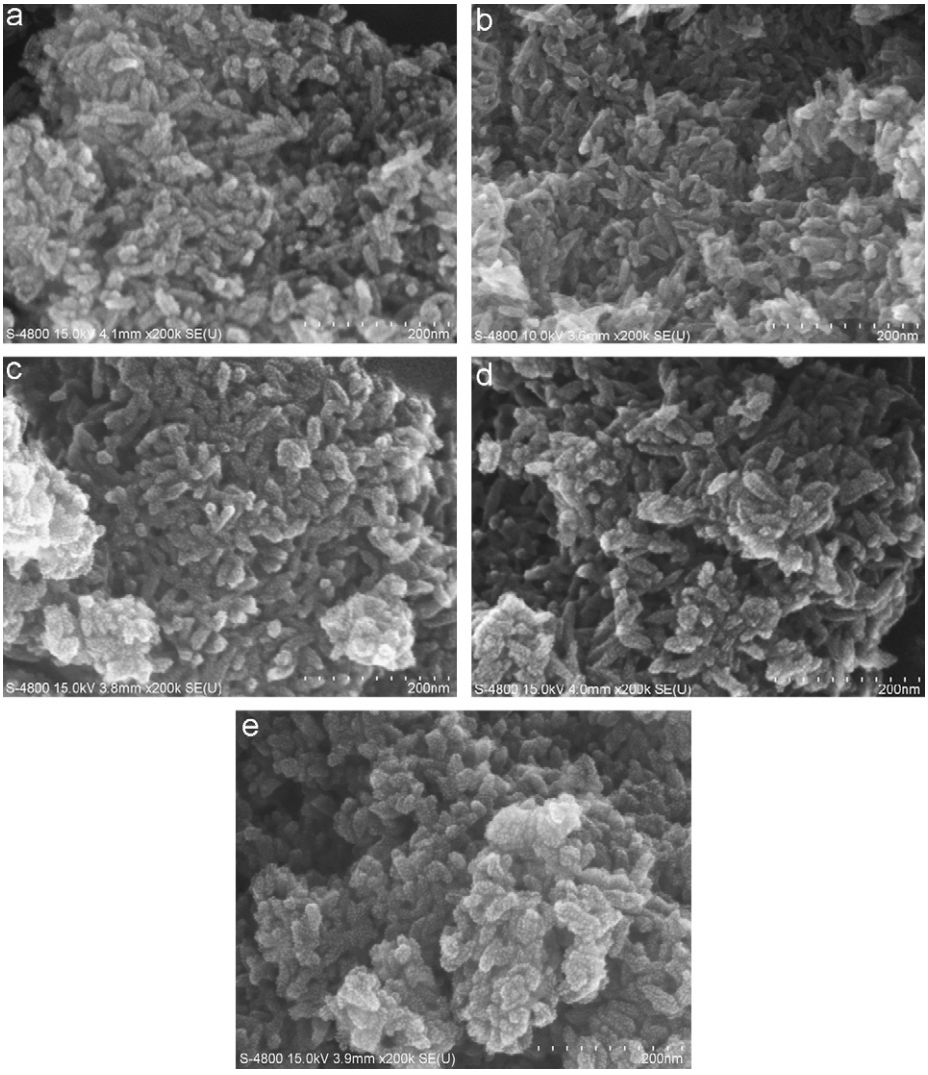

Fig. 3. High magnification FE SEM images of the F–N-codoped TiO_2 prepared with different starting CTAB concentrations: (a) 0 mM, (b) 0.1 mM, (c) 1 mM, (d) 10 mM and (e) 40 mM.

[30]. Sanchez and co-workers [31] have discussed the effect of different CTAB/Ti ratios on the structure of mesoporous of TiO_2 with high surface area of 280–370 $m^2 g^{-1}$. In the present work, we observed that yellow precipitates were formed when PTA solution was added into colorless and transparent aqueous solutions of CTAB and NH_4F. The higher the concentration of CTAB solution was, the sooner the precipitates presented, which indicated that the more CTAB enhanced the transformation from PTA to anatase TiO_2 particles. This conclusion is coincident with the XRD results shown in Fig. 2. In addition, the PTA micell might be bound to the micell group of CTAB, leading to a network structure during the formation of codoped anatase TiO_2 from PTA micell. The interaction between TiO_2 and CTAB resulted in the mesoporous structure after CTAB was removed by ethanol washing repeatedly.

X-ray photoelectron spectroscopy (XPS) survey spectrum (not shown here) indicated that F–N-codoped TiO_2 photocatalysts contain predominantly Ti, O, N and F elements and a trace amount of carbon. Fig. 7 represents the high-resolution XPS spectra of the Ti 2*p*, O 1*s*, F 1*s* and N 1*s* region, taken on the sample prepared with starting CTAB concentration of 10 mM. By calculating, the total surface concentrations of Ti, O, F and N were estimated to be 28.7, 65.2, 2.4, and 3.7 at%, respectively. The spin–orbit components ($2p_{3/2}$ and $2p_{1/2}$) of Ti 2*p* peaks are well deconvoluted by two curves at 458.9 and 464.6 eV (Fig. 7a) with a split of 5.7 eV between the doublets, indicating that Ti exists in the Ti^{4+} form [32]. The O 1*s* signal is shown in Fig. 7b. By curve fitting, the peak at 530.3 eV corresponds to lattice oxygen of TiO_2, and a shoulder located at higher binding energy of 532.4 eV is assigned to mixed contributions from surface hydroxides [33].

The F 1*s* region is composed of two contributions (Fig. 7c). The main contribution at 685.0 eV can be assigned to F^- ions physically adsorbed on the surface of samples and the minor contribution at 686.8 eV attributed to the doped F atoms in TiO_2, which is similar with that of some literatures [34]. The N 1*s* XPS spectrum shown in Fig. 7d also reveals a large broadness, which can be deconvoluted by two peaks with the binding energies at 400.2 and 401.9 eV and has been assigned to N in NO_x species by many researchers [35–37].

Fig. 8 compares the UV–vis DRS of F–N-codoped TiO_2 powders prepared with varying starting CTAB concentrations over the wavelength range of 250–650 nm. The codoping of nitrogen and fluorine resulted in a new obvious absorption band in the visible range, suggesting that the resulting samples can be activated by visible light. Furthermore, the absorption edge of new band shifted toward higher wavelength on the whole with increasing CTAB concentration. For example, the sample prepared with CTAB concentration of 10 mM showed visible-light absorption up to 600 nm.

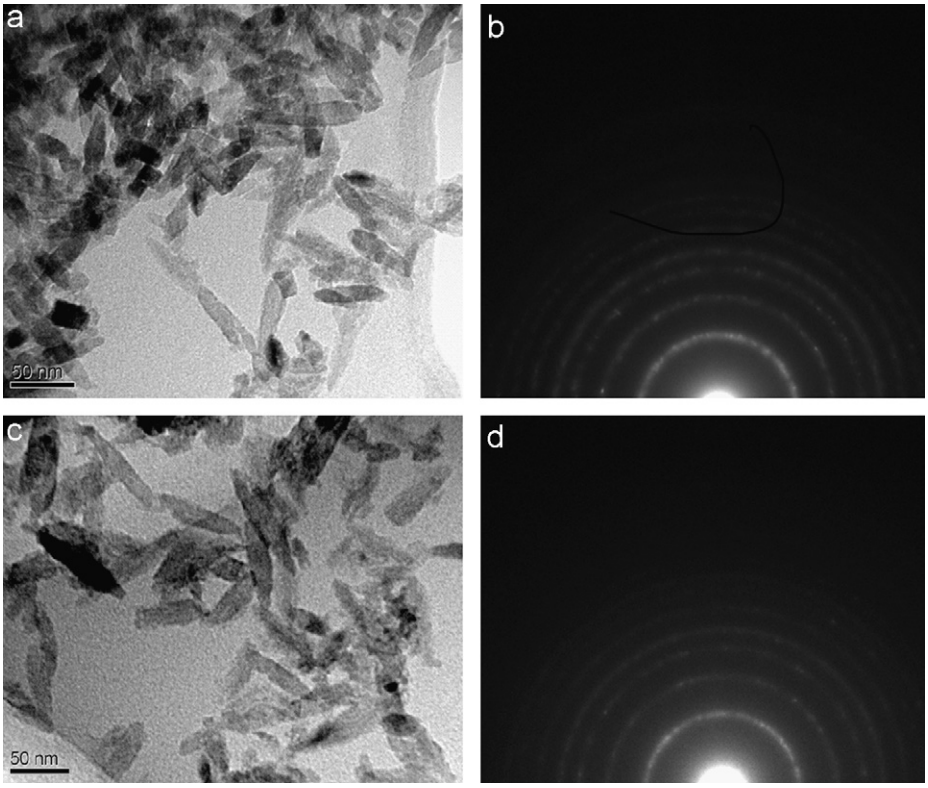

Fig. 4. TEM bright-field images of F–N-codoped TiO_2 prepared with starting CTAB surfactant of 0 mM (a, b) and 10 mM (c, d).

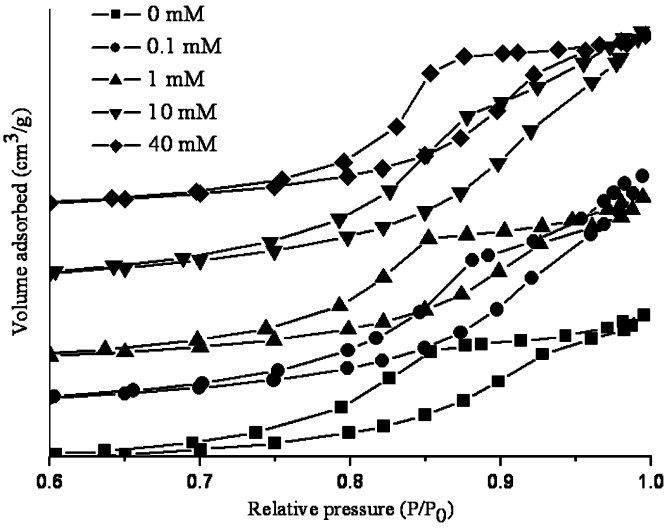

Fig. 5. Nitrogen adsorption–desorption isotherms of the F–N-codoped TiO_2 photocatalysts prepared at different CTAB concentrations.

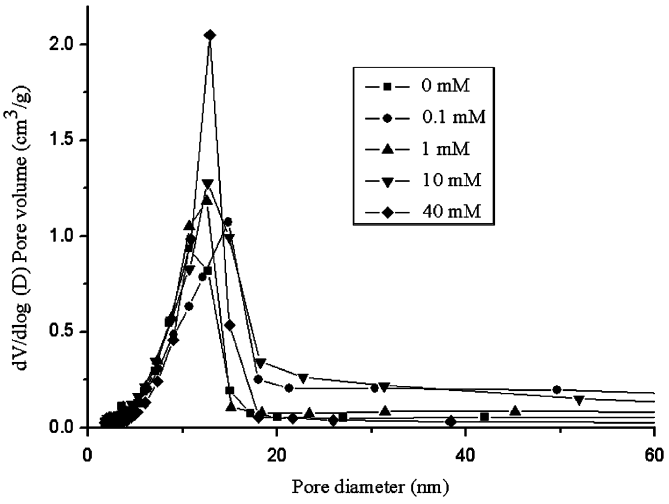

Fig. 6. Pore size distributions of F–N-codoped TiO_2 prepared with different CTAB concentrations derived from the desorption branches using the BJH method.

The significant red shift of the F–N-codoped TiO_2 powders clearly indicates a much decrease in the band gap energy of the as-prepared samples. Fig. 8 inset gives the plots of transformed Kubelka-Munk function versus the band gap energy. The extrapolation of the linear portion of the modified spectra to zero absorption determines the band gap energies of the as-prepared photocatalysts. In fact, there was F–N-induced midgaps for the codoped TiO_2, which were roughly estimated to be 2.3–2.6 eV for the samples prepared with 0.1–40 mM CTAB concentration.

F-doping was reported not to cause shift in the fundamental absorption edge of TiO_2 [38], while in other case the spectral absorption of the F-doped TiO_2 was found to show a stronger absorption in the UV–visible range and a red shift [34]. The mechanism of visible-light responses for N-doped TiO_2 is also under debate. Uhm and co-workers [39] concluded that the red shift in optical energy gap by N doping occurred because the energy level for N_{2p} state lied below the conduction band and valence band edge of TiO_2. Nakato and co-workers [40] reported the mechanism that visible-light responses for N-doped TiO_2 arised from formation of an N-induced (occupied) midgap level slightly above the valence band edge. Sakatani and co-workers [41] have attributed the visible responses to the paramagnetic nitrogen species (such as NO, NO_2, etc.). According to the analysis

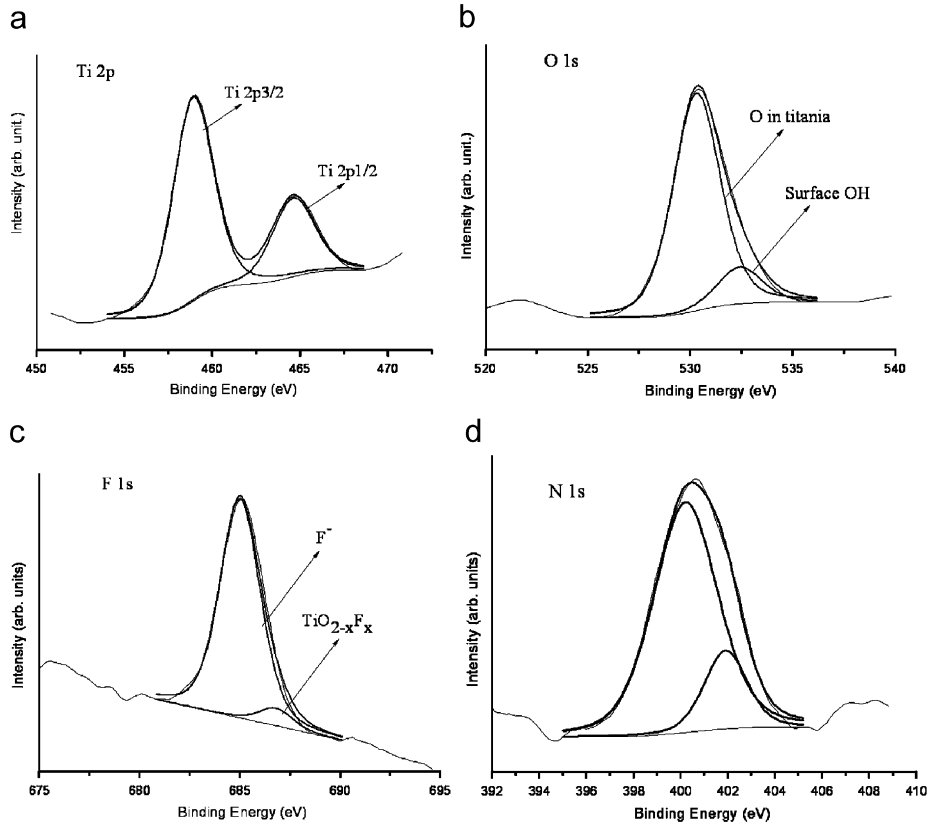

Fig. 7. Ti 2*p* (a), O 1*s* (b), F 1*s* (c) and N 1*s* (d) high-resolution XPS spectra of samples as-prepared with starting CTAB concentration of 10 mM.

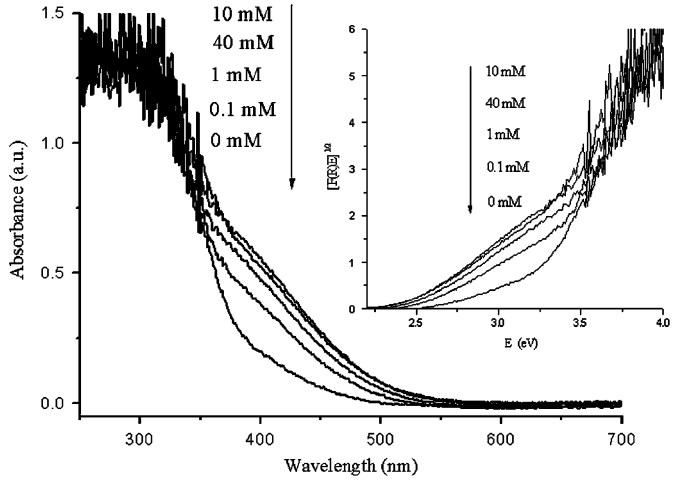

Fig. 8. UV–vis diffuse reflectance spectra and plot of the modified Kubelka-Munk (KM) function versus photon energy (*E*) for the reflectance spectra (inset) of F–N-codoped TiO_2 prepared with different CTAB concentrations.

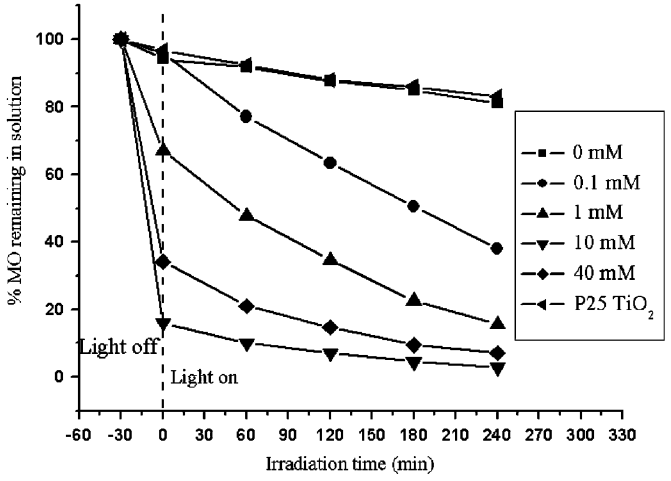

Fig. 9. Photocatalytic degradation curves of MO under visible light irradiation in the presence of the F–N-codoped TiO_2 photocatalysts and P25 TiO_2.

of XPS, the prominent visible light response shown in Fig. 8 might be the synergetic effects of doping F atoms in TiO_2 and NO_x species.

3.2. *Visible-light-induced catalytic activity studies*

The photocatalytic degrading curves are displayed in Fig. 9. It was found that after the powder samples have been dispersed into the MO aqueous solution for 30 min under no light irradiation, a decrease in the concentration of MO solution occurred, which was attributed to the adsorption of the TiO_2-based powders for MO molecules. This adsorption was greatly enhanced with increasing dosages of surfactant CTAB, for example, the sample prepared with starting CTAB concentration of 10 mM showed more than 20 times higher adsorption capacity for MO solution than P25 TiO_2. Table 1 shows that the relative coefficients (R) for all the products were close to 1, suggesting that the degradation of MO in the presence of the photocatalysts was first-order kinetics reaction. The slopes of the lines (not shown here) obtained by fitting linear $\ln(C_0/C)$ via irradiation time (t) could be considered as the photodegradation reaction rate constants. These rate constants

indicated that the F–N-codoped TiO_2 prepared with CTAB exhibited excellent visible-light activities for photodegradation of MO, which increased overall with increasing reactive CTAB concentration. Among them, the F–N-codoped sample prepared with CTAB concentration of 10 mM achieved the highest photodegradation activity with a MO conversion of 92.9% and 97.2% after 2 and 4 h irradiation, respectively, which was more than six times higher than that by Degussa P25 TiO_2. The increase in the photocatalytic activities of the sample prepared with CTAB might be owing to the improvement of visible-light absorption and red shift shown in Fig. 8 and the improvement of mesoporous structure.

4. Conclusion

In summary, we reported the preparation of F–N-codoped TiO_2 powders with mesoporous structure and good anatase crystallinity via sol–gel route using CTAB as surfactant for the first time. F–N-codoping resulted in a new absorption band, which shifted towards higher wavelength on the whole with increasing CTAB concentration. The results showed that the photocatalysts possessed a homogeneous pore diameter and a high surface area of 106.3–160.7 $m^3 g^{-1}$. The sample prepared with starting CTAB concentration of 10 mM showed an obvious spectral absorption up to 600 nm, and had more than six times higher photocatalytic activity and more than 20 times higher adsorption capacity for MO solution than those of P25 TiO_2. The present photocatalytic system with mesoporous F–N-codoped TiO_2 might be a good candidate to convert abundant visible or solar light energy into useful chemical energy.

Acknowledgments

This research was financially supported by the Program for Changjiang Scholars and Innovative Research Team in University (PCSIRT no. IRT0547) and the Cultivation Fund of the Key Scientific and Technical Innovation Project (no. 705036), Ministry of Education.

References

[1] F. Schüth, Chem. Mater. 13 (2001) 3184–3195.
[2] D. Chandra, N.K. Mal, M. Mukherjee, A. Bhaumik, J. Solid State Chem. 179 (2006) 1802–1807.
[3] S. Pavasupree, Y. Suzuki, S. Pivsa-Art, S. Yoshikawa, J. Solid State Chem. 178 (2005) 128–134.
[4] Y. Izumi, K. Konishi, M. Tsukahara, D.M. Obaid, K.-I. Aika, J. Phys. Chem. C 111 (2007) 10073–10081.
[5] P. Krawiec, S. Kaskel, J. Solid State Chem. 179 (2006) 2281–2289.
[6] D.M. Antonelli, Y.J. Ying, Angew. Chem. Int. Ed. Engl. 34 (1995) 2014.
[7] H. Choi, E. Stathatos, D.D. Dionysiou, Appl. Catal. B—Environ. 63 (2006) 60–67.
[8] H. Shibata, H. Mihara, T. Mukai, T. Ogura, H. Kohno, T. Ohkubo, H. Sakai, M. Abe, Chem. Mater. 18 (2006) 2256–2260.
[9] Y. Cho, W. Choi, Environ. Sci. Technol. 35 (2001) 966–970.
[10] H. Tada, T. Ishida, A. Takao, S. Ito, Langmuir 20 (2004) 7898–7900.
[11] R. Asahi, T. Morikawa, T. Ohwaki, A. Aoki, Y. Taga, Science 293 (2001) 269–271.
[12] Y.Z. Li, D.S. Hwang, N.H. Lee, S.J. Kim, Chem. Phys. Lett. 404 (2005) 25–29.
[13] R. Beranek, H. Kisch, Electrochem. Commun. 9 (2007) 761–766.
[14] A. Ghicov, J.M. Macak, H. Tsuchiya, J. Kunze, V. Haeublein, L. Frey, P. Schmuki, Nano Lett. 6 (2006) 1080–1082.
[15] L. Körösi, S. Papp, I. Bertóti, I. Dékány, Chem. Mater. 19 (2007) 4811–4819.
[16] A. Hattori, M. Yamamoto, H. Tada, S. Ito, Chem. Lett. 27 (1998) 707.
[17] L. Körösi, A. Oszkó, G. Galbács, A. Richardt, V. Zöllmer, I. Dékány, Appl. Catal. B 77 (2007) 175–183.
[18] K. Nukumizu, J. Nunoshige, T. Takata, J.N. Kondo, M. Hara, H. Kobayashi, K. Domen, Chem. Lett. 32 (2003) 196–197.
[19] Y. Xie, Y.Z. Li, X.J. Zhao, J. Mol. Catal. A: Chem. 277 (2007) 119–126.
[20] P. Calza, E. Pelizzetti, K. Mogyorósi, R. Kun, I. Dékány, Appl. Catal. B: Environ. 72 (2007) 314–321.
[21] T. Peng, A. Hasegawa, J. Qiu, K. Hirao, Chem. Mater. 15 (2003) 2011–2016.
[22] H. Shibata, T. Ogura, T. Mukai, T. Ohkubo, H. Sakai, M. Abe, J. Am. Chem. Soc. 127 (2005) 16396–16397.
[23] K. Cassiers, T. Linssen, M. Mathieu, Y.Q. Bai, H.Y. Zhu, P. Cool, E.F. Vansant, J. Phys. Chem. B 108 (2004) 3713–3721.
[24] D.Y. Wang, R.A. Caruso, F. Caruso, Chem. Mater. 13 (2001) 364–371.
[25] P.D. Cozzoli, A. Kornowski, H. Weller, J. Am. Chen. Soc. 125 (2003) 14539–14548.
[26] Y.W. Jun, M.F. Casula, J.H. Sim, S.Y. Kim, J. Cheon, A.P. Alivisatos, J. Am. Chem. Soc. 125 (2003) 15981–15985.
[27] G. Pacheco-Malagón, Norma A. Sanchez-Flores, J. Saniger-Blesa, L. Baños, P. Pérez-Romo, J.S. Valente, María de L. Guzman-Castillo, F. Hernández-Beltrán, J.J. Hernández-Beltrán, Micropor. Mesopor. Mater. 100 (2007) 70–76.
[28] P. Fabrizioli, T. Bürgi, A. Baiker, J. Catal. 207 (2002) 88–100.
[29] T. Sreethawong, Y. Yamada, T. Kobayashi, S. Yoshikawa, J. Mol. Catal. A: Chem. 241 (2005) 23–32.
[30] H. Shibata, T. Ogura, T. Mukai, T. Ohkubo, H. Sakai, M. Abe, J. Am. Chem. Soc. 127 (2005) 16396–16397.
[31] G.J. de A.A. Soler-Illia, A. Louis, C. Sanchez, Chem. Mater. 14 (2002) 750–759.
[32] B.M. Reddy, K.N. Rao, G.K. Reddy, P. Bharali, J. Mol. Catal. A: Chem. 253 (2006) 44–51.
[33] B. Erdem, R.A. Hunsicker, G.W. Simmons, E.D. Sudol, V.L. Dimonie, M.S. El-Aasser, Langmuir 17 (2001) 2664–2669.
[34] J.C. Yu, J.G. Yu, W.K. Ho, Z.T. Jiang, L.Z. Zhang, Chem. Mater. 14 (2002) 3808–3816.
[35] H. Chen, A. Nambu, W. Wen, J. Graciani, Z. Zhong, J.C. Hanson, E. Fujita, J.A. Rodriguez, J. Phys. Chem. C 111 (2007) 1366–1372.
[36] C. Chen, H. Bai, C. Chang, J. Phys. Chem. C 111 (2007) 15228–15235.
[37] S. Joung, T. Amemiya, M. Murabayashi, K. Itoh, Appl. Catal. A: General 312 (2006) 20–26.
[38] D. Li, H. Haneda, N.K. Labhsetwar, S. Hishita, N. Ohashi, Chem. Phys. Lett. 401 (2005) 579–584.
[39] Y.C. Hong, C.Uk. Bang, D.H. Shin, H.S. Uhm, Chem. Phys. Lett. 413 (2005) 454–457.
[40] R. Nakamura, T. Tanaka, Y. Nakato, J. Phys. Chem. B. 108 (2004) 10617–10620.
[41] Y. Sakatani, J. Nunoshige, H. Ando, K. Okusako, H. Koike, T. Takata, J.N. Kondo, M. Hara, K. Domen, Chem. Lett. 32 (2003) 1156.